J. Fluid Mech. (1985), *vol.* 16, *pp.* 405–424
Printed in Great Britain

A transformation for the energy-transfer term in isotropic turbulence

By L. CROCCO
Via Annia 16, 00184 Roma

AND P. ORLANDI
Dipartimento di Meccanica e Aeronautica, Università di Roma, La Sapienza,
Via Eudossiana, 16 00184 Roma

(Received 16 July 1983 and in revised form 10 December 1984)

The application of a particular transformation to the triadic integral results in an expression having the following advantages: (*a*) it satisfies global energy conservation in an evident fashion, independently of the accuracy of the energy-spectrum calculations; (*b*) it allows an economy of computational time; (*c*) it shows certain symmetries in the behaviour of non-local interactions; (*d*) it provides, for the non-local interactions contribution to the transfer function, an expression which is simpler and more compact than those existing, in spite of being more nearly complete; (*e*) finally the calculated energy-transfer distribution is in good agreement with the experimental findings through a very large range of R_λ.

1. Introduction

From a practical point of view, the Simple Reynolds-average description of turbulent boundary-layer flows is often considered sufficient for engineers. However, from a fundamental point of view, there is no doubt that the calculation of the actual turbulent solution of the Navier–Stokes equations is desirable. Unfortunately the existing procedures suited to this calculation are, computationally, so heavy that at the present stage they can be applied only in extremely limited circumstances, irrelevant to engineering requirements. This is, in particular, true for the appealing spectral approach where the turbulent fluctuations as well as their correlations are Fourier-transformed from the physical $\boldsymbol{x}$-space to the wavevector $\boldsymbol{k}$-space, thus resulting in substantial simplification of the equations for the velocity correlation spectra and for the spectrum $E(\boldsymbol{k})$ of the turbulent kinetic energy. Even in the simplest, isotropic case when E is a function only of k and there is only one equation to be solved, (1), the computational load involved in the calculation of the rate of energy transfer per unit wavenumber between different wavenumbers through the so-called triadic (or bipolar, or convolution) integral, (2), may still be too heavy in extreme conditions.

A substantial effort has been, and is being, made in order to reduce the computation time of the triadic integral without sacrificing the accuracy, accuracy being considered important in relation to the need to satisfy the global energy conservation. At low Reynolds number R_λ, when the spectrum is narrow, the number of calculation points in the integration area of the triadic integral necessary to reach the desired accuracy may still be acceptable, as, for instance, in the numerical integration scheme of Leith

& Kraichnan (1972). However, the spectrum widens when R_λ increases so that the necessary number of of points, and with it the computation time, increases substantially. In an effort to overcome the difficulty Lesieur & Schertzer (1972) have used the area integration of Leith & Kraichnan (1972), only on a smaller integration region, and have calculated the effects on the remaining cutoff areas by a specific procedure (to which we will come back later) thus succeeding in reducing the computation time.

The present authors have developed a different procedure which succeeds in lowering the computation time and presents other advantages. It is based on a transformation which changes the integration area from infinite to finite and allows the eventual reduction of the accuracy required in order to guarantee energy conservation. In addition it allows a better physical comprehension of certain compensations in the energy transfer between wavenumber triads. The advantages of the transformation apply in the most general case. Here, however, we shall restrict our considerations to the isotropic case.

2. The transformation of the energy equation

For isotropic turbulence the energy spectrum is a solution of Lin's equation

$$\frac{\partial E(k)}{\partial t} + 2\nu k^2 E(k) = T(k), \tag{1}$$

where $E(k)$ is related to mean turbulent energy corresponding to the velocity fluctuation $\boldsymbol{v}$ by

$$\tfrac{1}{2}\langle v^2 \rangle = \int_0^k E(k)\,\mathrm{d}k.$$

The expression for $T(k)$ is usually of the form

$$T(k) = \int_{\boldsymbol{p}+\boldsymbol{q}+\boldsymbol{k}=0} \Sigma(k,p,q)\,\mathrm{d}p\,\mathrm{d}q,$$

with the function Σ depending on the model. The functions E, T and Σ depend, of course, also on the time. The condition $\boldsymbol{p}+\boldsymbol{q}+\boldsymbol{k}=0$ means that the wavenumbers $\boldsymbol{p}$, $\boldsymbol{q}$ and $\boldsymbol{k}$ must form a triangle or, as usually stated, a triad. Explicitly one can write

$$T(k) = \int_0^\infty \mathrm{d}p \int_{|k-p|}^{|k+p|} \mathrm{d}q\, \Sigma(k,p,q). \tag{2}$$

Hence the integration area is a half-infinite strip on the (p, q)-plane, as shown in figure 1 (a). The integral is therefore the sum of its value T^+ calculated on the triangle to the left of the line $p = k$ and of its value T^- pertaining to the rest of the strip, to the right of $p = k$. Now for T^+ make the trivial substitution

$$p = \beta k, \quad q = \gamma k, \tag{3}$$

so that

$$\mathrm{d}p\,\mathrm{d}q = k^2\,\mathrm{d}\beta\,\mathrm{d}\gamma,$$

the limits of β and γ being

$$0 \leqslant \beta \leqslant 1, \quad 1-\beta \leqslant \gamma \leqslant 1+\beta.$$

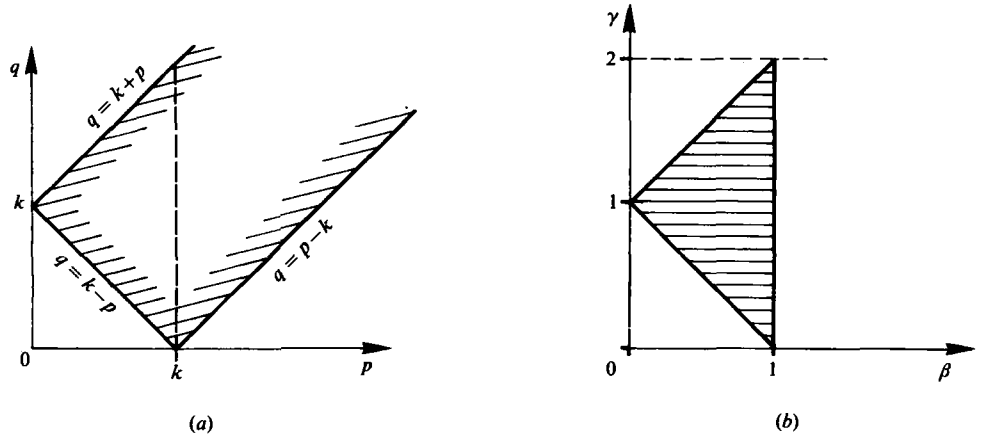

FIGURE 1. (*a*) Domain of integration in the (p, q)-plane.
(*b*) Domain of integration in the (β, γ)-plane.

For T^- apply a different substitution

$$k = \beta p, \quad q = \gamma p \quad \left(p = \frac{k}{\beta}, q = \frac{k\gamma}{\beta}\right) \tag{4}$$

so that

$$\mathrm{d}p\,\mathrm{d}q = -\frac{k^2}{\beta^3}\mathrm{d}\beta\,\mathrm{d}\gamma = -\frac{p^3}{k}\mathrm{d}\beta\,\mathrm{d}\gamma,$$

the limits of β and γ being the same as in the previous substitution. Observe that the triangles $(k, p, q)^+$ and $(p, k, q)^-$ are similar for β, γ assigned. Finally we have

$$T(k) = \frac{1}{k}\int_0^1 \mathrm{d}\beta \int_{1-\beta}^{1+\beta} \mathrm{d}\gamma\,[k^3\Sigma(k, \beta k, \gamma k) + p^3\Sigma(\beta p, p, \gamma p)], \tag{5}$$

with $p = k/\beta$; hence, in the plane (β, γ), the integration is to be performed only on the triangle of figure 1 (*b*).

In the EDQNM and in many other models Σ is given by

$$\Sigma(k, p, q) = k^3 pq\, B'(k, p, q)\, D'(k, p, q)\left[\frac{E(p)}{p^2} - \frac{E(k)}{k^2}\right]\frac{E(q)}{q^2}.$$

Here the geometrical factor B' is given by

$$B'(k, p, q) = \frac{p}{k}(xy + z^3),$$

x, y and z representing the cosines of the angles opposite respectively to k, p and q in the triadic triangle. D' is the 'relaxation frequency'; it comes out of the Markovianization of a certain integral with respect to t, and is given, for most models, by

$$D'(k, p, q) = \frac{1 - \mathrm{e}^{-[\eta(k)+\eta(p)+\eta(q)]t}}{\eta(k) + \eta(p) + \eta(q)},$$

the 'damping function' $\eta(k)$ depending on the model.

After transformation to the (β, γ)-plane we obtain

$$T(k) = \frac{1}{k}\int_0^1 \mathrm{d}\beta \int_{1-\gamma}^{1+\gamma} \mathrm{d}\gamma\,[S^+(k,\beta,\gamma) - S^-(k,\beta,\gamma)] = T^+(k) + T^-(k), \tag{6}$$

with

$$\left.\begin{aligned} S^+(k,\beta,\gamma) &= S(k,\beta,\gamma) = k^4 B(\beta,\gamma)\, D(k,\beta,\gamma)\left[\frac{E(\beta k)}{\beta^2} - E(k)\right]\frac{E(\gamma k)}{\gamma^2}, \\ S^-(k,\beta,\gamma) &= S\left(\frac{k}{\beta},\beta,\gamma\right). \end{aligned}\right\} \tag{7}$$

Here the geometrical factor is

$$B(\beta,\gamma) = \beta\gamma B' = 2\beta^2\gamma(xy + z^3),$$

the expression $xy + z$ taking the same value after the application of the substitution (3) and (4) because of the similitude of the two triadic triangles.

The result is

$$\begin{aligned} B(\beta,\gamma) &= \frac{\beta}{4\gamma}[\gamma^4 - (1-\beta^2)^2] + \frac{\gamma}{8\beta}(1+\beta^2-\gamma^2)^3 \\ &= \beta\gamma\left[1 - \left(\frac{1+\gamma^2-\beta^2}{2\gamma}\right)\right]\left[1 - \frac{\gamma^2}{2} - \frac{\gamma^2(1-\gamma^2)}{2\beta^2}\right]. \end{aligned} \tag{8}$$

B vanishes on the two sides $\gamma = 1 \pm \beta$ of the integration area, and on the curve $\beta^2 = \gamma^2(1-\gamma^2)/(2-\gamma^2)$ within the same area.

We have also from D' the relaxation frequency

$$D(k,\beta,\gamma) = \frac{1 - \mathrm{e}^{-[\eta(k)+\eta(\beta k)+\eta(k\gamma)]t}}{\eta(k) + \eta(\beta k) + \eta(\gamma k)}. \tag{9}$$

Clearly, the function (7), as well as $S(k/\beta, \beta, \gamma)$, vanishes on the perimeter of the domain of integration.

The transformation we have applied to obtain (6) for the transfer function, can also be used on the so-called energy flow (defined below) with the result

$$\Pi(k) = \int_k^\infty T(k_1)\,\mathrm{d}k_1 = \int_0^1 \mathrm{d}\beta \int_{1-\gamma}^{1+\gamma} \mathrm{d}\gamma\left[\psi(k,\beta,\gamma) - \psi\left(\frac{k}{\beta},\beta,\gamma\right)\right] = \Pi^+(k) + \Pi^-(k)$$

with

$$\psi(k,\beta,\gamma) = \int_k^\infty S(k_1,\beta,\gamma)\,\mathrm{d}\ln k_1.$$

The global energy conservation condition, expressed by

$$\int_0^\infty T(k)\,\mathrm{d}k = 0,$$

is immediately seen to be satisfied from (6) and (7) after inverting the order of the integrations, since for fixed β and γ $\mathrm{d}\ln l = \mathrm{d}\ln(k/\beta)$. The fact that the present form for $T(k)$ satisfies energy conservation without requiring T^+ and T^- to be computed with extreme accuracy certainly represents a substantial advantage of the proposed transformation. For the conservation it is sufficient that S be taken as the same function in the evaluation of T^+ and T^-, no matter how accurately this function has been determined. It is only important that, when $S(k,\beta,\gamma)$ is known, say, at discrete

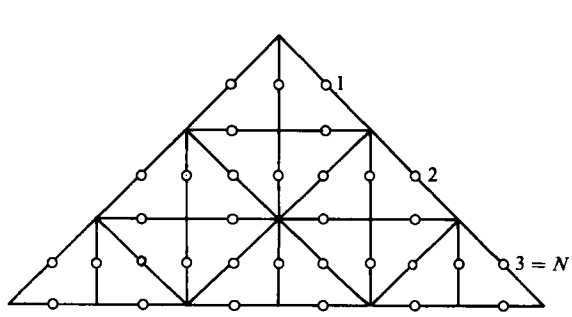

FIGURE 2. Discretization of the domain of integration.

values of $\log k$, the interpolation to obtain $S(k/\beta, \beta, \gamma)$ be properly performed. And, of course, this applies also to the calculation of $\psi(k, \beta, \gamma)$ or of

$$\int_k^a S\left(\frac{k_1}{\beta}, \beta, \gamma\right) \mathrm{d} \ln \frac{k_1}{\beta},$$

if a check of the energy-conservation condition, although unnecessary, is desired. In this case one must bear in mind that what one is checking is the interpolation and integration procedures, rather than the energy-conservation condition.

3. Numerical scheme

The principal aim of the applications presented in this section is the verification of the advantage of the present transformation. Its potential for reducing the computation time was investigated, but only partially; a deeper investigation was deferred to a succeeding paper. Simultaneously its possibilities with respect to the so-called non-local interactions were examined.

The discretization of the energy equation (1) followed the Herring–Kraichnan (1972) scheme

$$E(k, t_{n+1}) = \mathrm{e}^{-2\nu k^2 \Delta t} E(k, t_n) + \frac{1 - \mathrm{e}^{-2\nu k^2 \Delta t}}{2\nu k^2} T_m(k, t_n),$$

where different definitions of $T_m(k, t_n)$ can be used. For instance, Cambon, Jaendel & Mathieu (1981) have used the definition $T_m(k, t_n) = T(k, t_n)$. The maximum value of Δt for this explicit technique is, however, severely limited. Better results are obtained with Herring & Kraichnan's (1972) implicit scheme

$$T_m(k, t_n) = \tfrac{1}{2}[T(k, t_n) + T(k, t_{n+1})]$$

and solving it by the predictor–corrector technique.

The integration domain was discretized using the scheme of figure 2. Here the triangle of figure 1 (*b*) has been subdivided into $2N^2$ equal elementary triangles by splitting each of the two equal sides in N parts. In the figure $N = 3$. According to a known rule, if the function to be integrated is quadratic in β and γ, its mean value on each elementary triangle is the arithmetic mean of the values at the middle points of the three sides. This simple rule has been used as an approximation in the actual case. The general result for

$$I = \int_0^1 \mathrm{d}\beta \int_{1-\beta}^{1+\beta} G(\beta, \gamma) \, \mathrm{d}\gamma$$

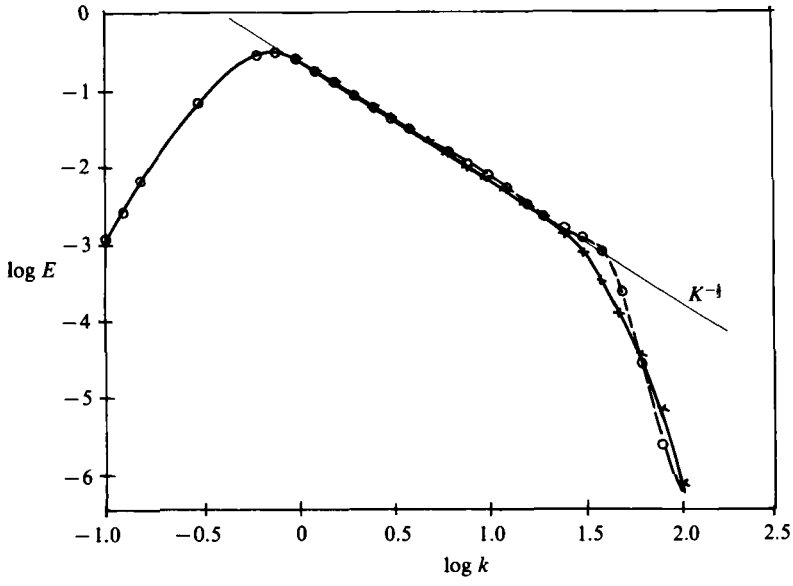

FIGURE 3. Energy spectra obtained for $F = 1$ (–○–) or $F = 3$ (–×–). $R_\lambda = 140$, $N = 10$.

is

$$I \approx \frac{1}{3N^2}\left[\sum_{i=1}^{N-1}\sum_{J=1}^{2i} G\left(\frac{i}{N}, 1+\frac{2J-2i-1}{2N}\right)+\sum_{i=0}^{N-1}\sum_{J=0}^{4i} G\left(\frac{2i+1}{2N}, 1+\frac{J-2i}{2N}\right)\right]$$
$$+\frac{1}{6N^2}\left[\sum_{i=1}^{2N} G\left(1, \frac{2i-1}{2N}\right)+\sum_{i=1}^{N} G\left(\frac{2i-1}{2N}, 1-\frac{2i-1}{2N}\right)+\sum_{i=1}^{N} G\left(\frac{2i-1}{2N}, 1+\frac{2i-1}{2N}\right)\right].$$

This general expression is simplified when calculating T^+, T^- or T; in which case one must take $G(\beta,\gamma) = S(k,\beta,\gamma)$ or $S(k/\beta,\beta,\gamma)$ or their difference, all three quantities vanishing, as noticed previously, on the perimeter of the domain of integration, so that I is reduced to the first two sums.

The discretization we have used has the advantage of a second-order accuracy for the same number of points as first-order accuracy obtained with the usual logarithmic discretization. However it has the drawback of requiring interpolations. These were performed to obtain good accuracy by the time-consuming cubic-spline technique. A comparison for equal accuracy between the two types of discretization is planned for future work.

Of course, the number F of points per octave of the log k discretization may have a noticeable effect on the accuracy, particularly in certain regions. This is clearly seen from figure 3, where the two curves of log E were obtained at $R_\lambda = 140$ with $N = 10$ and $F = 1$ or 3 respectively. It appears that due to the interpolation procedure an $F < 3$ may be a source of substantial oscillations and errors in particularly sensitive regions, such as the transition to the dissipative region.

The choice of N is only a matter of accuracy. Figure 4 shows the profiles of $kT(k)$ calculated at $R_\lambda = 840$ with $N = 3$, 5 and 10. It appears that $N = 3$ is definitely too low, while the transition from 5 to 10 has minor effects, except when kT is close to a peak. Observe that the number of necessary interpolations is at most 115 for $N = 5$ and 980 for $N = 10$. But the important thing is that, despite the inaccuracy resulting

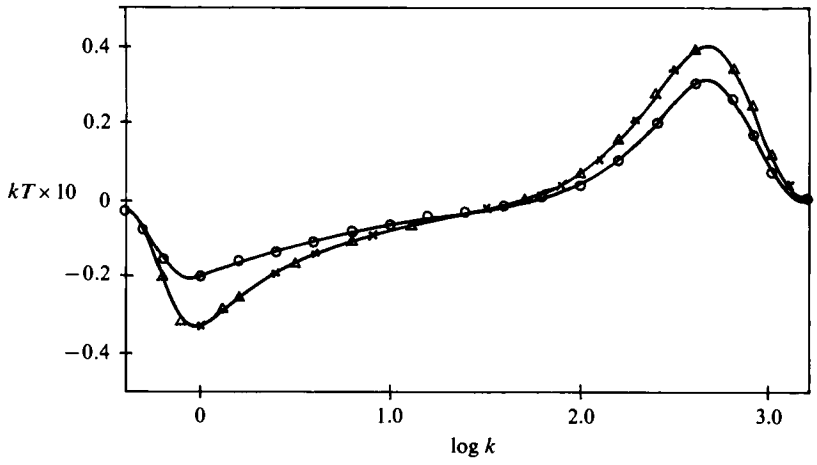

FIGURE 4. Distribution of $kT(k)$ obtained with $N = 3$ (–○–), $N = 5$ (–×–).

from a low N, the energy conservation is satisfied equally well in the three cases. This seems to be a positive achievement of the present transformation, as already noticed in §3.

4. Applications

The procedure outlined above has been systematically applied using the EDQNM model to a certain number of cases for which calculations have been performed by other authors using different models or techniques. The common features were: prescribed values of $R_\lambda(0)$ and a similar initial energy distribution given by

$$E(k,0) = E_p\left(\frac{k}{k_p}\right)^4 e^{2(1-k^2/k_p^2)},$$

where E_p indicates the peak value of E and k_p the corresponding wavenumber. The resulting initial Reynolds number $R(0)$ is $1.5216R_p$, $R_p = (1/\nu)(E_p/k_p)^{\frac{1}{2}}$ being the Reynolds number corresponding to the energy peak which must be properly chosen in order to obtain the prescribed $R_\lambda(0)$ with an assigned ν. Usually this is achieved by properly choosing the value of ν leaving E_p and k_p unchanged.

The expression of $\eta(k)$ generally adopted for the EDQNM model (Pouquet, Lesieur & André 1975; Lesieur & Schertzer 1977; Cambon *et al.* 1981) is

$$\eta_1(k) = \nu k^2 + \lambda_1\left(\int_0^k k_1^2 E(k_1)\,\mathrm{d}k_1\right)^{\frac{1}{2}}, \tag{10}$$

with $\lambda_1 \approx 0.355$–0.360.

For the limited purposes of the present investigation we have often chosen to use the simpler expression of Orszag (1970)

$$\eta_2(k) = \nu k^2 + \lambda_2[k^3 E(k)]^{\frac{1}{2}}, \tag{11}$$

except when discussing precisely the influence of the η choice. For $E(k)$ the two expressions coincide provided $\lambda_2 = \lambda_1(\frac{2}{3})^{\frac{1}{2}}$. This would suggest the value $\lambda_2 = 0.307 \div 0.312$. However, because of an oversight the value used in the present application was $\lambda_2 = \lambda_1 = 0.360$.

The examples go from low to very high $R_\lambda(0)$.

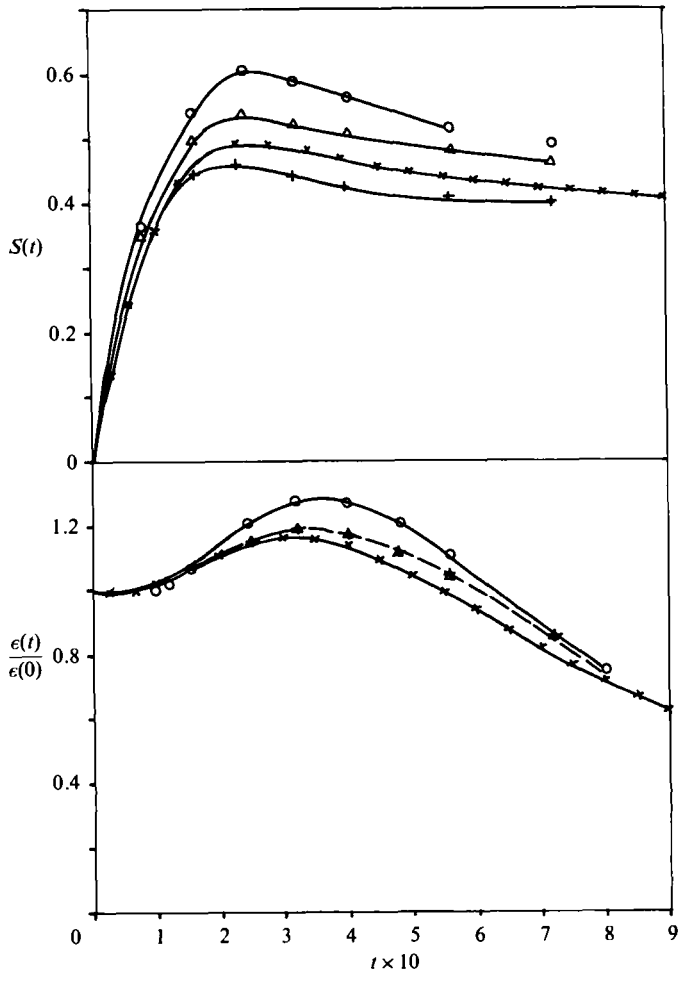

FIGURE 5. Distribution of $S(t)$ and $\epsilon(t)/\epsilon(0)$ resulting from different models or procedures, (–O–) TFM, (–+–) DIA, (–×–) EDQNM, with $\eta_2(11)$, (–△–) Direct Simulation (Orszag & Patterson). $R_\lambda(0) = 35$.

4.1. *Low* $R_\lambda(0)$

Herring & Kraichman (1972) have compared the results obtained with TFM and DIA with the results of DS by Orszag & Patterson (1972) for many cases starting from different initial spectra, among which was the initial spectrum considered here, with different R_λ. We have calculated here with the EDQNM and (11) for $\mu(k)$ the case when $R_\lambda(0) = 35$. The calculations that follow were obtained with $N = 10$. Figure 5 shows the behaviour of the skewness and the total dissipation. Our results are comparable with those of Herring & Kraichnan (1972). Our skewness matches the values obtained from DS better.

4.2. *Mean* $R_\lambda(0)$

This is the case calculated by Newman & Herring (1979) with the TFM method applied to the diffusion of a passive scalar. Here we shall consider only their results related to the energy spectrum and compare them with the results we obtain using the EDQNM method and (11) for $\eta(k)$. The initial $R_\lambda(0)$ is 200. Figures 6 (*a–b*) show the comparison

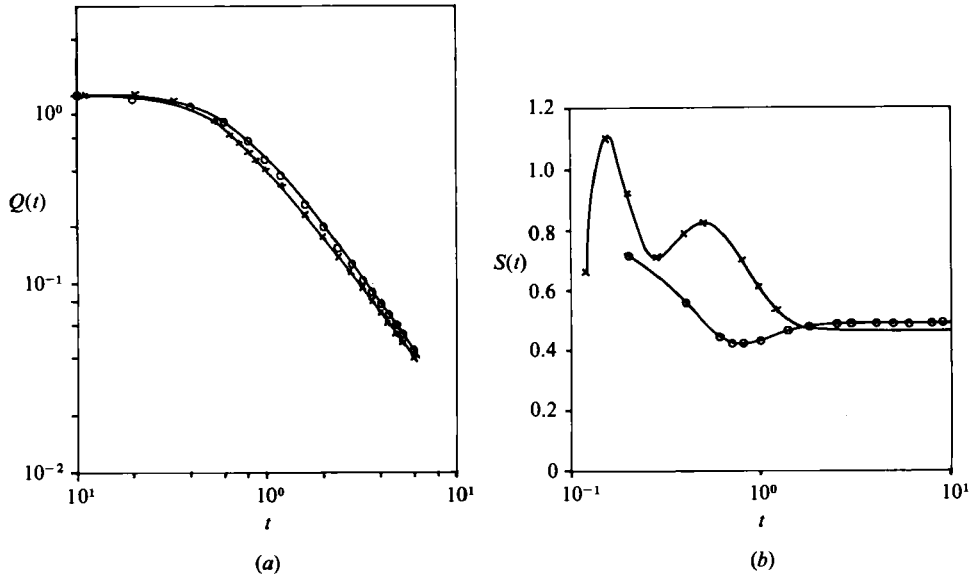

FIGURE 6. (*a*) Total kinetic energy $Q(t)$, obtained with $R_\lambda(0) = 200$. (*b*) Skewness $S(t)$, obtained with $R_\lambda(0) = 200$, (–○–) TFM, (–×–) EDQNM.

concerning the developments of $Q = \frac{1}{2}\langle v \rangle$ and the skewness S as functions of t. For the first quantity the comparison is quite favourable with the exception of a difference in the duration of the initial phase, necessary to achieve an equilibrium condition. In equilibrium, approximating by $Q \sim t^{-n}$, n is 1.40 for the EDQNM and 1.38 for the TFM. The experimental value of Yeh & Van Atta (1973) is 1.34. For the other two quantities there are important differences (especially for S) during the initial phase. However, the comparison is very good once equilibrium is attained.

4.3. *High and very high* $R_\lambda(0)$

The two cases considered here are those studied by André & Lesieur (1977) relative to $R = Q^{\frac{1}{2}}/(\nu k_p) = 813$ and 32800. The corresponding $R_\lambda(0)$ are 1330 and 53500.

We are presenting this time more details (available, of course, also in the previous cases with analogous results, but not presented here) in order to support the statement we made at the end of §1 about the help our transformation provides for the physical comprehension of the interactions. Figure 7 shows the values of kT^+, kT^- and kT for $N = 3$, 5, 10 for $R_\lambda(0) = 1330$ and $t = 6.0$. Even the last value is far from sufficient to ensure the proper evaluation of $T^\pm$. However, the kT values appear to be properly evaluated.

The corresponding structure of the triadic interaction is represented in figure 8 (*a–d*). The isolevel plots of S^+ and S^- are shown on the plane β, γ for four values of k and $N = 10$. Of course, both quantities vanish, with $B(\beta, \gamma)$, on the periphery of the domain of integration, and on a particular line within this area. For sufficiently low values of β, $S^\pm$ can reach appreciable positive peaks, with a tendency to have roughly symmetrical negative peaks in the region $\lambda > 1$. Another positive peak is found near the corner $\beta = 1$, $\gamma = 0$ where, when γ is sufficiently small, $S^\pm$ can take appreciable values in spite of the low values of B. Substantially lower values are observed when β is close to 1 and $\gamma > 1$ in spite of the high value of B. Observe that in the figures

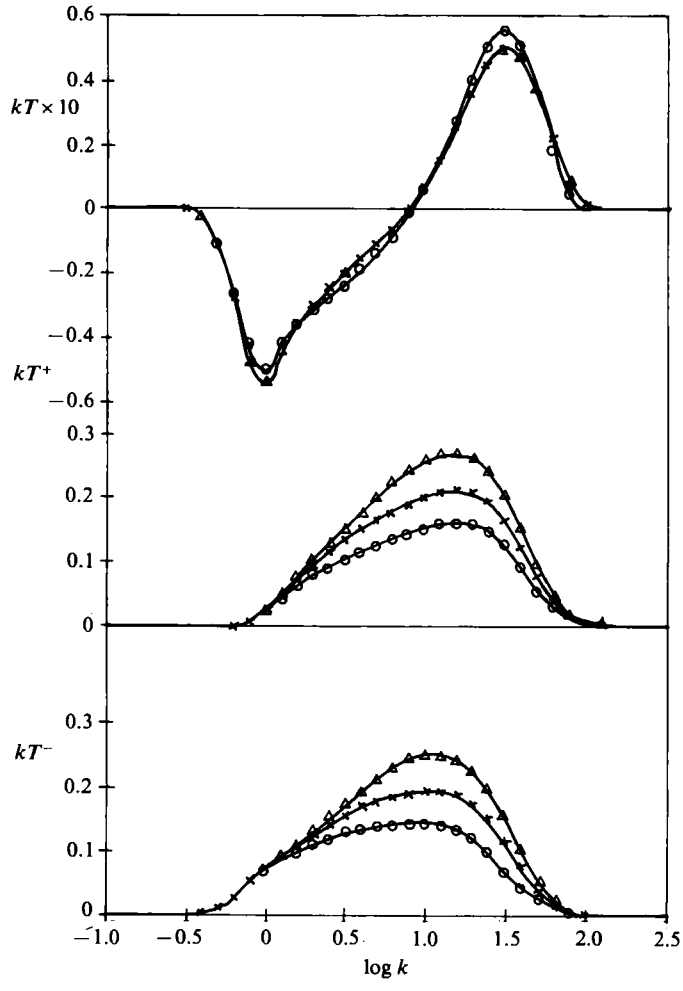

FIGURE 7. Distribution of $kT^{\pm}$ and kT, obtained with $N = 3$ (−○−), $N = 5$ (−×−), $N = 10$ (−△−), $R_\lambda(0) = 1330$, $t = 6.0$, $R_\lambda = 140$.

some of the peaks may become too feeble to appear on the isolevel plots. However, it is a simple matter to calculate approximate locations for the peaks in every case.

They are shown in the figures by crosses. At low k they are quite inaccurate with respect to the approximate numerically obtained positions. The accuracy improves at high k.

The roughly antisymmetrical behaviour of $S^{\pm}$ when β is small has the result that when calculating the integral in γ appearing in (6) the contributions from positive and negative portions have a tendency to cancel each other. In other words between the two regions $\gamma \gtrless 1$ there is, for small β, an intense transfer of energy which does not appear finally in $T^{\pm}$. Similarly for small γ the contributions from the highest values of S^+ almost cancel those of S^-. Hence there is an intense transfer of energy between the + and − regions which, after integration, does not appear in $T = T^+ - T^-$.

The trends appearing at $R_\lambda(0) = 1330$ are confirmed at $R_\lambda(0) = 53500$. The isolevel plots of $S^{\pm}$ are not reported here. They are similar to the previous ones, but with

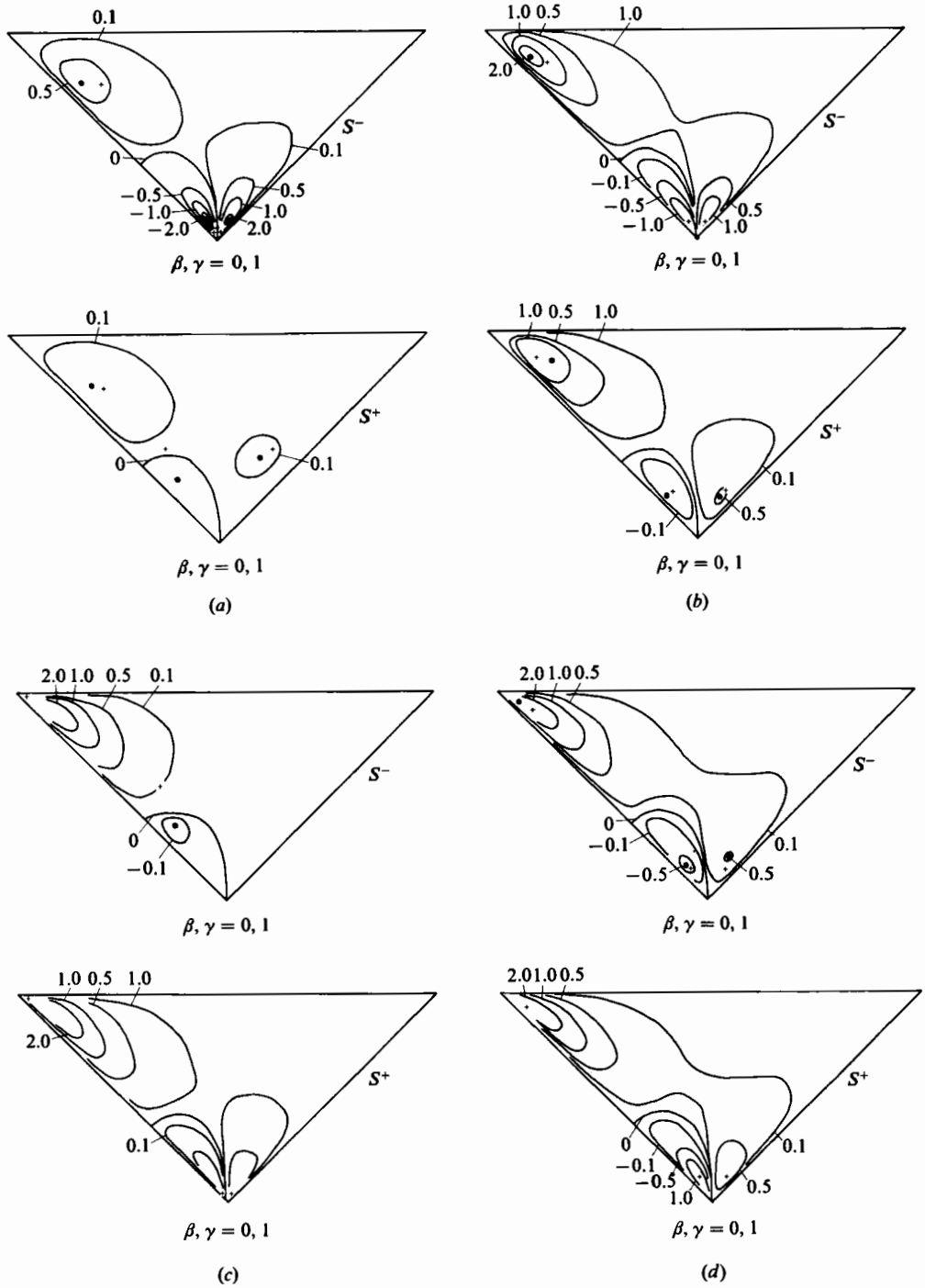

FIGURE 8. Isolevel plots of $S^{\pm}$ with $R_\lambda(0) = 1330$, $t = 6$, $R_\lambda = 140$ at (*a*) $\log k = 0$, (*b*) $\log k \simeq 0.5$, (*c*) $\log k \simeq 0.8$, (*d*) $\log k \simeq 1.4$.

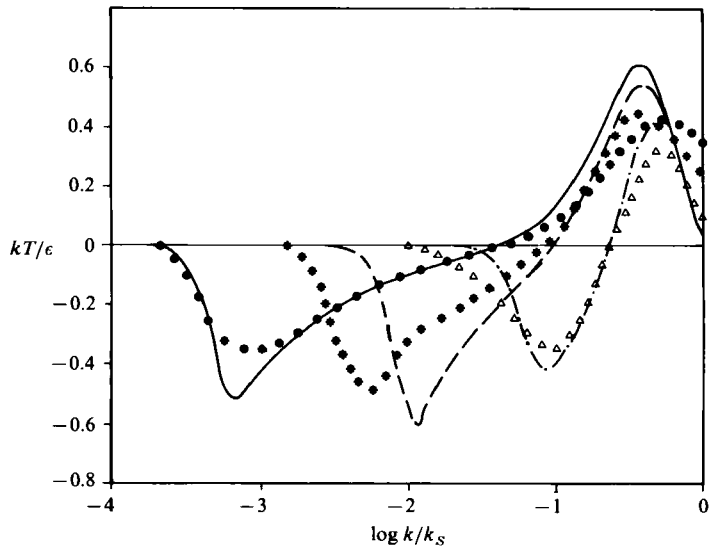

FIGURE 9. Distribution of $kT(k)/\epsilon$. Comparison between computed (——, $R_\lambda = 840$; – – –, $R_\lambda = 137$; –·–·–, $R_\lambda = 35$) and experimental values (●, $R_\lambda = 951$; *, $R_\lambda = 240$; △, $R_\lambda = 35$).

the widening of the k-range the peaks come closer to the points $\beta = 0$ and $\gamma = 0$, and their magnitude tends to increase, thus increasing the integration problems. For instance, the maximum value of $S^{\pm}$ for $\gamma \ll 1$ is found around $\gamma = 0.006$ and $\beta = 0.996$ and is 150 times larger than their values at $\gamma = 0.1$, $\beta = 0.95$.

4.4. *Comparison with experimental results*

It would be, of course, quite interesting to be in possession of experimental results relative to the distribution of the energy-transfer rate among all possible triads. Such results are not available, and even simpler results, such as those concerning $T(k, k')$ which represents the net transfer between two spherical wavenumber shells (as suggested by Helland, Van Atta & Stegun), have not been obtained.

The only thing we can compare on figure 9 is the distributions of the global transfers $T(k)$ with those obtained by Helland *et al.* (1977) in the same range of R_λ.

The computed curves show the expected collapse of the curves of kT/ϵ (ϵ = dissipation) around $k_s = (\epsilon/\nu^3)^{\frac{1}{4}}$. The experimental curves do not exhibit a similar collapse, probably because of experimental difficulties. The general shape of the curves is quite similar, with maxima and minima predicted within the same uncertainties as those reported by Helland *et al.* (1977) when deriving the experimental values in two different ways. Observe that, as found experimentally, the so-called inertial range does not correspond to almost vanishing $T(k)$, although the $k^{-\frac{5}{3}}$ behaviour is followed almost perfectly over a rather wide range (see figure 3 for $R_\lambda = 140$).

4.5. *Effect of the damping formula*

We found it instructive to compare at these R_λ the results obtained with the two different $\eta(k)$ expressions η_1 (10) and η_2 (11). In addition we have computed with the simplified expression

$$D = \frac{1}{\eta(k) + \eta(\beta k) + \eta(\gamma k)}, \tag{12}$$

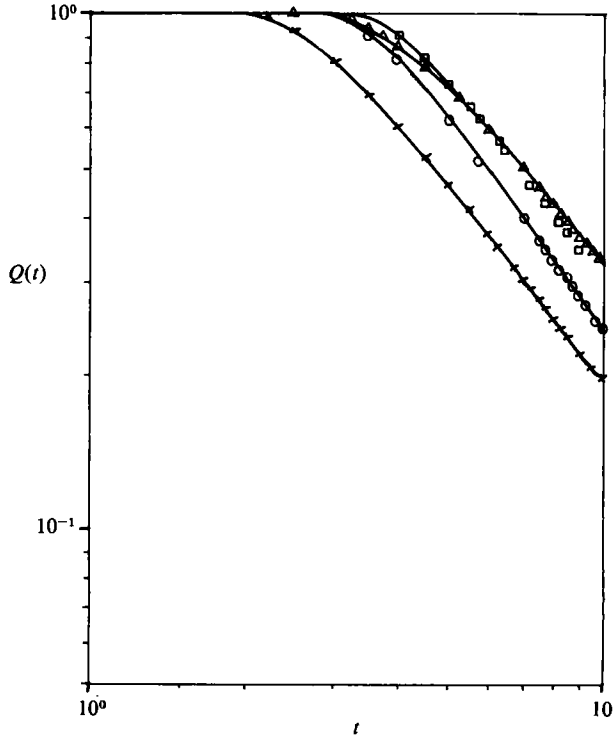

FIGURE 10. Total energy $Q(t)$ resulting from EDQNM with different $\eta(k)$ and D given by: $-\bigcirc-$, equations (10), (9); $-\triangle-$, equations (11), (9); $-\times-$, equations (10), (12); $-\square-$, equations (12), (15).

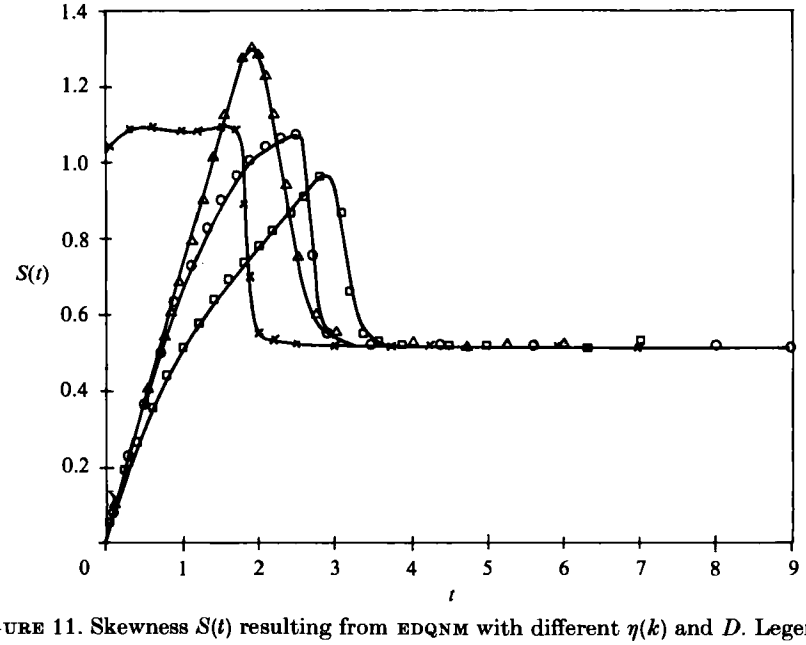

FIGURE 11. Skewness $S(t)$ resulting from EDQNM with different $\eta(k)$ and D. Legend as figure 10.

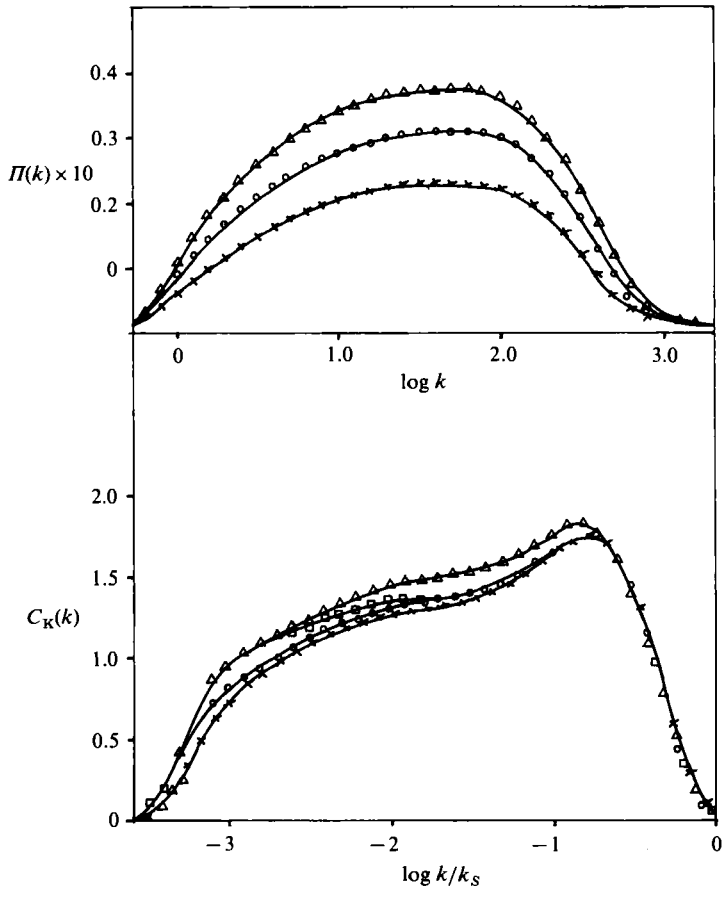

FIGURE 12. Transport power $\Pi(k)$ and Kolmogoroff coefficient $E(k)k^{\frac{5}{3}}\epsilon/3$ resulting from EDQNM with different $\eta(k)$ and D. Legend as figure 10.

obtained by suppressing the exponential at the numerator of (9) and with the other simplified expression,

$$D = \frac{t}{1+[\eta(k)+\eta(\beta k)+\eta(\gamma k)]\,t}, \tag{13}$$

suggested by Pouquet *et al.* (1975). To our knowledge this comparison has never been presented in literature. The results are reported in figure 10, where the values of the total turbulent energy $Q(t)$ are shown. It is clear that the suppression of the exponential in (12) for D has the effect of producing a premature drop of Q. We see that the results with (9) and (10), or (13) and (12) are appreciably different, contradicting the statements of Pouquet *et al.* (1975). The results obtained with (9) and (11) appear to be close to the latter ones.

The damping function and the relaxation-frequency expression have a more important effect in the higher-wavenumber regions, as shown by the strong effects on $S(t)$ from figure 11. Equation (12) produces a flat initial region, in contrast with the results of the other cases. This might be the cause of the poor prediction obtained by Cambon *et al.* (1981) when compared with the experiments of Compte-Bellot & Corrsin (1971). Aupoix (private communication) reached the same conclusion. All

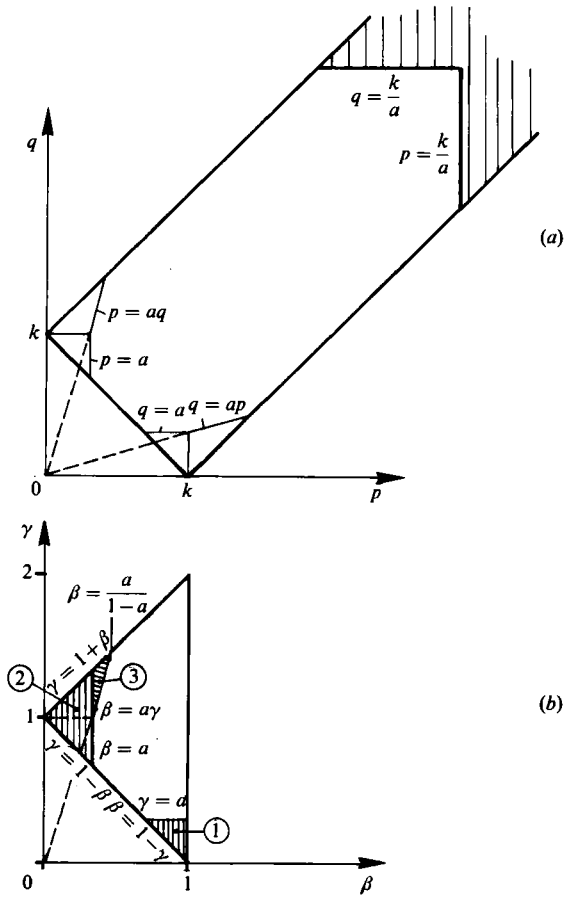

FIGURE 13. (*a*) Domain of integration in the (p, q)-plane for kT_{NL}. (*b*) Domain of integration in the (β, γ)-plane for kT_{NL}.

schemes predict the same asymptotic value for large times. Finally figure 12 shows the distribution of the Kolmogoroff coefficient $E(k)\, k^{\frac{5}{3}} \epsilon^{\frac{2}{3}}$ and of the transport power $\Pi(k)$. The differences are rather small among the Kolmogoroff coefficient distributions. In all cases an extensive inertial region is found, with the characteristic bump near the maximum positive kT. Larger differences are present among the transport power distributions.

4.6. *Non-local interactions*

The distributions of $S^{\pm}$ show that difficulties appear in the process of integration necessary to obtain $kT^{\pm}$ when R_λ increases, because the wavenumber range becomes wider and high peaks appear at low β or γ. The corresponding contributions to the integrals appear to be due to interactions between the two wavenumbers of comparable magnitude and one much smaller. They are generally indicated as non-local interactions. In an effort to save computation time when calculating these interactions, Lesieur & Schertzer (1977) following a suggestion of Kraichnan (1976) used narrower cutoff limits, associated with a particular analytical procedure for the evaluation of the non-local interactions.

Here we will show that the Lesieur & Schertzer technique may be applied with advantage to our transformed energy equation (6). We choose a small scale ratio a and we call non-local interactions those for which

$$\frac{\inf(k,p,q)}{\sup(k,p,q)} < a.$$

With the usual formulation in the (p,q)-plane, this means that we have to calculate the contribution to the double integral (2) of the shaded area of figure 13 (a). For the transformed integral (6), the integration area for the non-local interactions is given by the shaded area of figure 13 (b). The lower one, 1, corresponds to small values of γ and $\beta_0 = 1-\beta$, the upper one, split into 2 and 3, to small β and $\gamma_0 = \gamma - 1$. Area 3 has been included for the sake of completeness, since it is a consequence of the inequality above. It is included in the developments of Lesieur & Schertzer. But in our opinion its contribution should be disregarded if (as in our case) the numerical integration leaves out only the areas $\gamma \leqslant a$ (area 1) and $\beta \leqslant a$ (area 2).

The result for the contribution T_{NL} is given by

$$kT_{\mathrm{NL}} = kT_1 + kT_2 + kT_3.$$

Here

$$\left.\begin{aligned} kT_1 &= \int_0^a \mathrm{d}\gamma \int_0^\gamma \mathrm{d}\beta_0 \left[S(k, 1-\beta_0, \gamma) - S\left(\frac{k}{1-\beta_0}, 1-\beta_0, \gamma\right)\right], \\ kT_2 &= \int_0^a \mathrm{d}\beta \int_{-\beta}^{\beta} \mathrm{d}\gamma_0 \left[S(k, \beta, 1+\gamma_0) - S\left(\frac{k}{\beta}, \beta, 1+\gamma_0\right)\right], \\ kT_3 &= \int_a^{a/(1-a)} \mathrm{d}\beta \int_{\beta/a-1}^{\beta} \mathrm{d}\gamma_0 \left[S(k, \beta, 1+\gamma_0) - S\left(\frac{k}{\beta}, \beta, 1+\gamma_0\right)\right]. \end{aligned}\right\} \tag{14}$$

The computation is straightforward. For small β_0 or γ_0 we develop the integrand in corresponding powers and perform the second integral of the above expressions. The complete results are given in the Appendix, from which we transcribe only the equations for areas 1 and 2 according to our observation above:

$$kT_1 = \int_0^a \gamma^2 \tau_1(k,\gamma)\,\mathrm{d}\gamma + O(a^m),$$

$$kT_2 = \int_0^a \beta^2 \left[\tau_2(k,\beta) - \tau_2\left(\frac{k}{\beta}, \beta\right)\right] \mathrm{d}\beta + O(a^n).$$

With the complete expressions given in the Appendix for τ_1 and τ_2 we have $m = 6$, $n = 7$, so the error may be quite small even for a not far from unity. However, the complete expressions require the calculation of derivatives with respect to k, β, γ up to a third order of E and D, a troublesome task. If, however, the last term of the expressions of τ_1 and τ_2 is dropped a fortunate cancellation takes place and only first-order derivatives survive, while the value of m and n drops to 5, which is still a very satisfactory value. The corresponding expressions for τ_1 and τ_2 are reported here:

$$\tau_1(k,\gamma) = k\left[\frac{2}{15}\frac{\partial}{\partial k}(k^4 X_0) + \frac{\gamma}{24}\frac{\partial}{\partial k}(k^4 X_1)\right],$$

$$\tau_2(k,\beta) = \tfrac{4}{15} k^4 [E(\beta k) - \beta^2 E(k)]\, Y_0,$$

with the expressions for X_0, X_1 and Y_0 given in the Appendix.

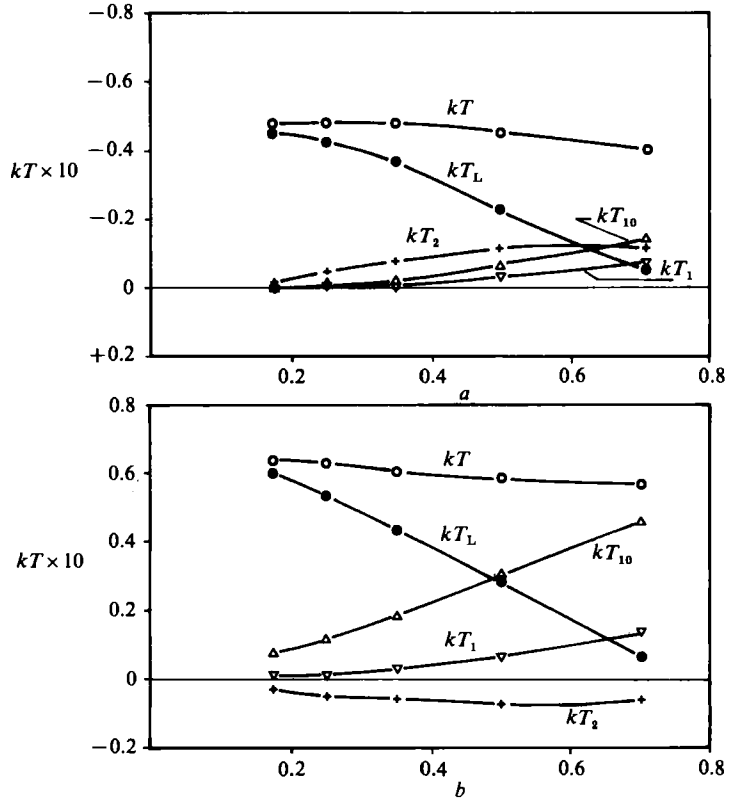

FIGURE 14. Behaviour of local, non-local and total energy transfer (*a*) $\log k = 0$; (*b*) $\log k = 1.66$.

To analyse the influence of the parameter a on the evaluation of the energy transfer, various calculations, based on the EDQNM closure, have been performed for the decay of isotropic turbulence of a flow with $R_\lambda(t = 0) = 1330$. The calculations have been made using four points per octave. Figure 14 shows the local, non-local and total energy transfer at $t = 6$ and at two values of k where kT reaches respectively the minimum and the maximum value. The non-local interactions due to the area 1 have been split in two parts: the first one kT_{10} due to the zeroth-order term in the expression of $\tau_1(k, \gamma)$ and kT_{11} due to the first-order term. At low k the effect of non-local interactions is smaller than the effect at high k. The contribution of the kT_{11} term, which was not considered by Lesieur & Schertzer, is sensible at high values of a as expected. The non-local interactions at high values of a overcome completely the effect of local interactions. At high k the non-local interactions due to area 2 have an opposite effect with respect to the interactions due to area 1. Although the local and non-local interactions terms show sensible variations with the parameter a, it is very important to notice that the total transfer kT remains almost constant up to substantial values of a. The use of very high values of a for the calculation allows a reduction of computational time. As already observed the kT_{11} term was not considered by Lesieur & Schertzer who kept only the lowest-order term of the development with the results that $m = n = 3$ only. It is also to be noticed that our expressions are more compact and easier to handle than those of Lesieur & Schertzer despite their being pushed to higher order and including the variation of D, which was taken as constant in their paper.

5. Conclusions

We have shown that a particular transformation of the infinite (p, q)-strip on which the triadic integral has to be performed produces a rather simple expression to be integrated on a finite area, with the result that faster calculations can be done. The most interesting aspect of the transformed integral is that when calculating numerically the transfer function T the energy conservation condition $\int_0^\infty T\,\mathrm{d}k = 0$ is automatically satisfied even when knowledge of the corresponding spectrum is not quite accurate. Accuracy, however, is an important requirement for the standard integration in the (p, q)-plane.

The transformed integrand consists of two parts, S^+ and S^-. At high R_λ (but even, to a certain extent, at low R_λ) these quantities present peaks in certain regions where one of the three wavenumbers of the triad is substantially smaller than the other two (non-local interactions). Due to certain symmetries of these peaks (clearly apparent in the transformed expressions) it appears that the effect of the peaks tend to cancel. This is verified by analytically computing the non-local interactions following the suggestion of Lesieur & Schertzer (1977). The resulting expressions are of a more compact and symmetrical form than those obtained by the above authors. In addition they are pushed to a higher order of accuracy and they include the variations of D (which was kept constant by the above authors). The use of our non-local corrections may substantially reduce the overall T-computation time. It is also shown that the non-local corrections satisfy energy conservation by themselves.

Appendix

From (14), developing and integrating in β_0 we have

$$KT_1 = \int_0^a \gamma^2 \tau_1(k, \gamma)\,\mathrm{d}\gamma + O(a^7).$$

Here

$$\tau_1(k,\gamma) = \tfrac{2}{15}\bar{s}_\beta + \frac{\gamma}{24}(\bar{\bar{s}}_\beta - 3\bar{s}_\beta - \bar{s}_{\beta\beta}) + \frac{\gamma^2}{210}(2\bar{\bar{\bar{s}}}_\beta - 6\bar{\bar{s}}_\beta - 28\bar{s}_\beta - 3\bar{\bar{s}}_{\beta\beta} - 9\bar{s}_{\beta\beta} + 2\bar{s}_{\beta\beta\beta}),$$

where

$$s(k,\beta,\gamma) = k^4 D(k,\beta,\gamma)\left[\frac{E(\beta k)}{\beta^2} - E(k)\right] E(\gamma k)$$

and the superposed dots and the indices indicate partial derivatives with respect to $x = \ln k$ and to β while the superposed bar means that the derivatives are calculated at $\beta = 1$.

Switching the integration order we have to $O(a^5)$

$$\int_0^\infty T_1\,\mathrm{d}k = \int_0^a \gamma^2\,\mathrm{d}\gamma \int_{-\infty}^{+\infty} \tau_1(k,\gamma)\,\mathrm{d}x = 0,$$

since τ_1 can be expressed as the derivative with respect to x of an expression vanishing at the limits $\pm\infty$.

Similarly we obtain from (14), developing and integrating in γ_0,

$$kT_2 = \int_0^a \beta^2 \left[\tau_2(k,\beta) - \tau_2\left(\frac{k}{\beta}, \beta\right)\right] \mathrm{d}\beta + O(a^7),$$

$$kT_3 = \int_0^{a/(1-a)} \beta \left[\tau_3(k,\beta) - \tau_3\left(\frac{k}{\beta}, \beta\right)\right] \mathrm{d}\beta + O(a^6),$$

where

$$\tau_2(k,\beta) = k^4[E(\beta k)-\beta^2 E(k)]\,\{\tfrac{4}{15}(5\tilde{\sigma}+\tilde{\sigma}_\gamma)+\tfrac{1}{210}\beta^2(63\tilde{\sigma}+14\tilde{\sigma}_\gamma-44\tilde{\sigma}_{\gamma\gamma}-4\tilde{\sigma}_{\gamma\gamma\gamma})\},$$

$$\begin{aligned}\tau_3(k,\beta) = k^4[E(\beta k)-\beta^2 E(k)]\,\{&\tfrac{1}{4}(1-A^2)\,\tilde{\sigma}+\tfrac{1}{6}\beta(1-A^2)\,[(4+5A+6A^2+3A^3)\,\tilde{\sigma}\\&+(2+4A+6A^2+3A^3)\,\tilde{\sigma}_\gamma]\\&+\tfrac{1}{24}\beta^2\,(1-A^2)^2\,[3(3A^2-1)\,\tilde{\sigma}+2(4+5A^2)\,\tilde{\sigma}_\gamma+2(1+2A^2)\,\tilde{\sigma}_{\gamma\gamma}]\},\end{aligned}$$

where $$\sigma(k,\beta,\gamma) = D(k,\beta,\gamma)\,E(\gamma k)/\gamma^2, \quad A = 1/a-1/\beta$$

and the tilde indicates that σ and its partial derivatives are calculated at $\gamma = 1$.

Since $\mathrm{d}\ln k = \mathrm{d}\ln(k/\beta)$ it is evident, after inverting the integration order with respect to x and β, that to all orders

$$\int_0^\infty T_2\,\mathrm{d}k = \int_0^\infty T_3\,\mathrm{d}k = 0.$$

Altogether we have, within the order of the calculation,

$$\int_0^\infty T_{\mathrm{NL}}\,\mathrm{d}k = \int_0^\infty (T_1+T_2+T_3)\,\mathrm{d}k = 0,$$

which expresses energy conservation for the non-local corrections.

More explicit expressions for τ_1, τ_2 and τ_3 are the following obtained considering all quantities to be functions of $x = \ln k$, so that $\ln(\beta k) = x+b$, and $\ln(\gamma k) = x+c$, with $b = \ln\beta$ and $c = \ln\gamma$.

$$\tau_1 = k^4\,[\tfrac{2}{15}(\dot{X}_0+4X_0)+\tfrac{1}{24}\gamma(\dot{X}_1+4X_1)+\tfrac{1}{210}\gamma^2(\dot{X}_2+4X_2)],$$

with

$$\begin{aligned}X_0 &= (\dot{E}-2E)\,\bar{E}\bar{D},\\ X_1 &= (\dot{E}-2E)\,[(\dot{\bar{E}}+4\bar{E})\,\bar{D}+\bar{E}(\dot{\bar{D}}-2\bar{D}b)],\\ X_2 &= [(\dot{E}-2E)\,(2\ddot{\bar{E}}+19\dot{\bar{E}}+44\bar{E})+(\ddot{E}-22\dot{E}+63\dot{E}-46E)\,\bar{E}]\,\bar{D}\\ &\quad+[4(\dot{E}-2E)\,(\dot{\bar{E}}+2\bar{E})+(\ddot{E}+\dot{E}-6E)\,\bar{E}]\,\dot{\bar{D}}+2(\dot{E}-2E)\,\bar{E}\ddot{\bar{D}}\\ &\quad-6(\dot{E}-2E)\,[(\dot{\bar{E}}+11\bar{E})\,\bar{D}_b-\bar{E}\dot{D}_b+\bar{E}\bar{D}_{bb}].\end{aligned}$$

The derivatives of D are given by

$$\bar{D} = \bar{d}_0, \quad \dot{\bar{D}} = -\bar{d}_1(2\dot{\eta}+\dot{\bar{\eta}}), \quad \ddot{\bar{D}} = -\bar{d}_1(2\ddot{\eta}+\ddot{\bar{\eta}})+2\bar{d}_2(2\dot{\eta}+\dot{\bar{\eta}})^2,$$

$$\bar{D}_b = -\bar{d}_1\dot{\eta}, \quad \bar{D}_{bb} = -\bar{d}_1\ddot{\eta}+2\bar{d}_2\dot{\eta}^2, \quad \dot{\bar{D}}_b = -\bar{d}_1\ddot{\eta}+2\bar{d}_2\dot{\eta}(2\dot{\eta}+\dot{\bar{\eta}}),$$

with

$$\bar{d}_0 = \frac{1-\mathrm{e}^{-(2\eta+\bar{\eta})t}}{2\eta+\bar{\eta}}, \quad \bar{d}_1 = \frac{1-(1+2\eta+\bar{\eta})\,t\,\mathrm{e}^{-(2\eta+\bar{\eta})t}}{(2\eta+\bar{\eta})^2},$$

$$\bar{d}_2 = \frac{1-[1+(2\eta+\bar{\eta})\,t+\tfrac{1}{2}(2\eta+\bar{\eta})^2\,t^2]}{(2\eta+\bar{\eta})^3}\,\mathrm{e}^{-(2\eta+\bar{\eta})t}.$$

Here again the η are taken at x, the $\bar{\eta}$ at $x+c$. For τ_2 and τ_3 we obtain

$$\tau_2 = k^4[E(\beta k)-\beta^2 E(k)]\,(\tfrac{4}{15}Y_0-\tfrac{1}{210}\beta^2 Y_2),$$

$$\tau_3 = k^4[E(\beta k)-\beta^2 E(k)]\,(\tfrac{1}{4}Z_0+\tfrac{1}{6}\beta\,Z_1+\tfrac{1}{24}\beta^2\,Z_2),$$

where

$$Y_0 = (\dot{E}+3E)\,\tilde{D}+E\tilde{D}_c,$$

$$Y_2 = (4\ddot{E}+8\dot{E}-130\dot{E}-133E)\,\tilde{D}+2(6\ddot{E}+8\dot{E}-65E)\,\tilde{D}_c+4(3\dot{E}+2E)\,\tilde{D}_{cc}+4E\tilde{D}_{ccc},$$

$$Z_0 = (1-A^2)^2\,E\tilde{D},$$

$$Z_1 = (1-A)^2[(2+4A+6A^2+3A^3)\,(\dot{E}\tilde{D}+E\tilde{D}_c)-3A(1+A)^2\,E\tilde{D}],$$

$$Z_2 = (1-A^2)^2\,[2(1+2A^2)\,(\ddot{E}\tilde{D}+2\dot{E}\tilde{D}_c+E\tilde{D}_{cc}) - 2(1+5A^2)\,(\dot{E}\tilde{D}+E\tilde{D}_c)+(13A_2-7)\,E\tilde{D}],$$

with $A = 1/a-1/\beta$,

$$\tilde{D} = \tilde{d}_0;\quad \tilde{D}_c = -\tilde{d}_t\,\dot{\eta};\quad \tilde{D}_{cc} = -\tilde{d}_1\,\ddot{\eta}+2\tilde{d}_2\,\dot{\eta}^2;\quad \tilde{D}_{ccc} = -\tilde{d}_1\,\dddot{\eta}+6\tilde{d}_2\,\dot{\eta}\ddot{\eta}-6\tilde{d}_3\,\dot{\eta}^3;$$

the $\tilde{d}_0, \tilde{d}_1, \tilde{d}_2$ being given by the corresponding barred quantities with $\tilde{\eta} = \eta(x+b)$ in place of $\bar{\eta} = \eta(x+c)$ and $\tilde{d}_3$ by

$$\tilde{d}_3 = \frac{1-[1+(2\eta+\tilde{\eta})\,t+\frac{1}{2}(2\eta+\tilde{\eta})^2\,t^2+\frac{1}{6}(2\eta+\tilde{\eta})^3\,t^3]\,\mathrm{e}^{-(2\eta+\tilde{\eta})\,t}}{(2\eta+\tilde{\eta})^4}.$$

REFERENCES

André, J. C. & Lesieur, M. 1977 Influence of helicity on the evolution of isotropic turbulence at high Reynolds number. *J. Fluid Mech.* **81**, 187–207.

Cambon, C., Jaendel, D. & Mathieu, J. 1981 Spectral modelling of non-isotropic turbulence. *J. Fluid Mech.* **104**, 247–262.

Comte-Bellot, G. & Corrsin, S. 1971 Simple Eulerian time correlation of full- and narrow-band velocity signals in grid-generated isotropic turbulence. *J. Fluid Mech.* **48**, 273–337.

Helland, K. N., Van Atta, C. W. & Stegen, G. R. 1977 Spectral energy transfer in high Reynolds number turbulence. *J. Fluid Mech.* **79**, 337–359.

Herring, J. R. & Kraichnan, R. H. 1972 Comparison of some approximations for isotropic turbulence. In *Statistical Models and Turbulence* (ed. M. Rosenblatt & C. Van Atta). Lecture Notes in Physics vol. 12, pp. 146–194. Springer.

Kraichnan, R. H. 1976 Eddy viscosity in two and three dimensions, *J. Atmos. Sci.* **33**, 1521–1536.

Leith, C. E. & Kraichnan, R. H. 1972 Predictability of turbulent flows. *J. Atmos. Sci.* **29**, 1041–1058.

Lesieur, M. & Schertzer, D. 1977 Amortissement autosimilaire d'une turbulence à grand nombre de Reynolds. *J. Méc.* **17**, 607–646.

Newman, G. R. & Herring, J. R. 1979 A test field model study of a passive scalar in isotropic turbulence. *J. Fluid Mech.* **94**, 169–194.

Orszag, S. A. 1970 Analytical theories of turbulence. *J. Fluid Mech.* **41**, 363–386.

Orszag, S. A. & Patterson, G. S. 1972 Numerical simulation of three-dimensional homogeneous isotropic turbulence. In *Statistical Models and Turbulence* (ed. M. Rosenblatt & C. Van Atta). Lecture Notes in Physics vol. 12, pp. 127–145. Springer.

Pouquet, A., Lesieur, M. & André, J. C. 1975 High Reynolds number simulation of two-dimensional homogeneous isotropic turbulence using a stochastic model. *J. Fluid Mech.* **72**, 305–319.

Yeh, T. T. & Van Atta, C. C. 1973 Spectral transfer of scalar and velocity fields in heated grid turbulence. *J. Fluid Mech.* **58**, 233–263.